Micromaterials and Interfaces (2026) Volume 4 Issue 1
doi: 10.59429/mi.v4i1.15123

ARTS AND SCIENCE
ARTS AND SCIENCE PRESS PTE. LTD

RESEARCH ARTICLE

Lignin Extraction from Cotton Stalk and FTIR Analysis of Functional Group Evolution During Different Ranges of Thermal Treatment

Md. Sarwar Jahan, Md. Latifur Rahman, Faisal S. Rahaman, Samsur Rahaman, Mubarak Ahmad Khan*

Research Laboratory, Echotex Limted, Chandra Polli Biddut, Gazipur-1751, Bangladesh

***Corresponding author:** Mubarak Ahmad Khan, makhan.inst@gmail.com

ABSTRACT

Lignin is an abundant natural source for bio-oil and biopolymers. Lignin is an alternative source for natural carbon, graphite, graphene, and graphene oxide. In this research, lignin was extracted from cotton stalks via an alkali treatment, and changes in functional groups were measured at normal and high temperatures (0 to 1600ºC). In this temperature range, 0 to 200ºC, lignin showed a peak at 1710 cm-1 (C=O ketones, aldehydes, and carbonyls), guaiacyl/syyringyl aromatic skeleton at the 1608 cm-1 peak of C=C, and an ether linkage C-O-C at 1127 cm-1. At temperatures of 300-500ºC, it represents methoxy groups, carbonyls, and ether linkages. At 600ºC, the carbonyl group was eliminated from this treated sample. Aliphatic and oxygen were removed at 700- 1000ºC. In this region, the 2104 cm-1 peak denoted sp-hybridized carbon, the 2323 cm-1 peak indicated CO2 evolution, and the 1391 cm-1 peak gradually developed, indicating aromatic/sp2 carbon precursors related to carbon ordering in hierarchical graphene-like carbon. In the temperature range 1200 to 1600ºC, a few weak organic bands were observed, indicating the presence of near-graphitic sp2 graphite lattices. In the XRD analysis at 1600ºC represent, two theta values were 25.24º, 43.62º, 78.87º and the crystal plane (002), (100)/(101), (110) and 0.353 nm interlayer spacing (d_{002}) where Lc ≈ 0.9 nm; La ≈ 5 nm; ~3 layers; g ≈ 0 that conformed to the hexagonal turbostratic carbon. This hexagonal turbostratic carbon region has shown that it can be used in battery anodic materials, solar cell counter electrodes, and other highly conductive material applications.

Keywords: Lignin, Turbostratic Carbon, Thermal Properties, FTIR, Carbon Derivatives

ARTICLE INFO
Received: 04 September 2026| Accepted: 10 November 2026 | Available online: 27 November 2026

CITATION
Jahan, M.S., Rahman M.L., Rahaman F.S., Rahaman, S., Khan M.A.. Lignin Extraction from Cotton Stalk and FTIR Analysis of Functional Group Evolution During Different Ranges of Thermal Treatment. Micromaterials and Interfaces 2026; 4(1): 15123. doi: 10.59429/mi.v4i1.15123

COPYRIGHT
Copyright © 2026 by author(s). *Micromaterials and Interfacesis* published by Arts and Science Press Pte. Ltd. This is an Open Access article distributed under the terms of the Creative *Commons* Attribution License (https://creativecommons.org/licenses/by/4.0/), permitting distribution and reproduction in any medium, provided the original work is cited.

Highlights

- Lignin, extracted from cotton stalk using alkali treatment.
- Carbonyl (1710 cm^{-1}) and aromatic (1608 cm^{-1}) bands weakened by 600ºC.
- Solid yield decreased from 87% at 100ºC to 22% at 1600 ºC.
- FTIR was used for the follow-up of the functional groups of lignin thermal treatment in the range 100-1600ºC.
- XRD analysis confirmed that the carbon used in the synthesis of the turbostatic carbon is graphitic.

1. Introduction

Lignin is the second most abundant natural polymer on Earth after cellulose. Lignin is a complex three-dimensional aromatic macromolecule that represents up to 30% of the cell wall dry mass in vascular plants. Constituting about 15–30% of lignocellulosic biomass in dry weight, lignin is a large and underutilized source of renewable carbon. Consequently, the efficient recovery of lignin from biomass such as agricultural by-products has attracted significant scientific and industrial interest in terms of sustainable biobased economies and valorizing those residues [1]. Structurally, lignin is a highly heterogeneous polymer, comprised of three main phenylpropanoid monolignol units p-coumaryl alcohol, coniferyl alcohol, and sinapyl alcohol which are incorporated into the polymer as p-hydroxyphenyl (H), guaiacyl (G) and syringyl (S) units respectively. These monomers are interconnected by diverse ether (C-O-C) and carbon-carbon (C-C) linkages, with the β-O-4 aryl ether linkage being the most abundant source [2].

The complex and non-linear nature of this bonding network has endowed lignin with considerable chemical recalcitrance, so that its selective separation from the cellulose and hemicellulose rich components of biomass is technically difficult but industrially important. Lignin content in cotton stalks, non-woody lignocellulosic waste widely available in regions that practice extensive cotton cultivation, is generally between 18 and 25% (dry weight), making it a promising yet understudied feedstock [3]. Isolated lignin is a key process in the biorefinery concept where lignocellulosic biomass can be fractionated into its constituent components and converted into value-added products. Historically, lignin has been considered a waste product of the pulp and paper industry, stemming primarily from Kraft and sulfite pulping processes, and has been combusted on-site for energy recovery [4, 5]. However, plentiful supply combined with increasing awareness of the complex aromatic chemistry of lignin has led to exploration of using it as a feedstock for biofuels, bio-based chemicals (including vanillin and phenols), carbon fibers, adhesives, antioxidants and polymeric materials. Processes like soda pulping and organosolv extraction are promising for cotton stalks, given their adaptation to herbaceous biomass with low sulfonation degree lignin and maintained aromatic structure [6]. Various methods for lignin extraction have been developed, producing lignins with specific structural and chemical properties depending on the processing conditions applied, which significantly impact yield as well as the purity of the product and its functional group credibility. The most important types are Kraft pulping (use of NaOH and Na_2S at high temperature), sulfite pulping (lignosulfonates as a by-product), organosolv processes (e.g., on the basis of ethanol), soda pulping (alkaline, sulfur-free), and the emerging green methods, ionic liquids, steam treatment and particularly deep eutectic solvents (DES). Therefore, soda extraction was selected here, as it is a simple method which is well suited for herbaceous biomass and yielded lignin with a low degree of sulfonation and preserved aromatic structure. Other recent research related to lignin extraction and the production of lignin-derived carbons also applies to this work [5, 7, 8]. Lignin isolation methods have advanced, but challenges remain, for example, the variability of lignin from one species to another, and from one tissue to another, makes it difficult to come up with a standardized protocol, and harsh processing conditions can cause structural changes [9].

In this study, lignin from cotton stalks is extracted using an alkaline extraction method and the changes in the functional groups of the extracted lignin after thermal treatments are studied in the temperature range of 100-1600 °C and the solid yield after thermal treatment at each temperature is also studied. This aims to explain the evolution of FTIR active functional groups of cotton stalk lignin as a function of temperature-dependent structural changes. It is hypothesized that these groups are increasingly lost with increasing carbon content. These insights aim to enhance lignin yield and quality for high-value applications (e.g. energy storage, energy generation industries, stealth composites, and EMI shielding materials), advancing the circular bioeconomy [5, 10-12].

2. Material and Method

2.1. Material

Cotton Stalk collected from Dinajpur Cotton Research institute in Bangladesh, NaOH from local market in Bangladesh, Sulfuric Acid from BASF, Germany, distilled water from own laboratory, Ethanol from Mark India.

2.2. Method

2.2.1. Lignin Extraction from Cotton Stalk

Cotton Stalk were cut to 2mm then treated with a 2% (w/w) sodium hydroxide solution for 2 hours at 90°C, then cooled down to room temperature. 5% sulfuric acid was used to neutralize to these alkali solutions. After neutralization, lignin was separated from this aqueous solution and then filtered with a 45-micron sieve. The aqueous lignin was dried in the oven at 80°C then washed several times wash and dried for purification.

2.2.2. Thermal treatment

During the thermal treatment process dried lignin was ground with a mortar and pestle then sieved at a 20-micron mesh. 10gm of micro-sized lignin was placed into a crucible then placed in a vacuum furnace (model: TA2-4-17TP). After that, turn on the vacuum channel and turn on the vacuum pump, when the furnace vacuum -0.1MPa, turn-off the vacuum channel and turn-on the vacuum gas inlet channel. The nitrogen flow rate was ~10 liter/minutes where 99.994% pure nitrogen was used for this treatment. The heat treatment was vacuum nitrogen furnace in 100 to 1600°C for 3 hours, with a temperature gradient 5°C/min 100 to 1200°C and 4°C/min 1300-1600°C. When the reaction was done, the temperature gradually decreased 4°C/min until 30°C in a normal environment for cooling of the material. This reacted material was tested for conformation of turbostratic carbon and yield amount side by side.

3. Characterization

3.1. FTIR

The chemical functional groups of the extracted lignin, and its derivatives were analyzed using a Fourier-transform infrared (FTIR) spectrometer (Spectrum Two, PerkinElmer, UK) equipped with a lithium tantalate ($LiTaO_3$) detector and diamond ATR. The spectra resolution was used up to 0.5cm^{-1}, wavelength

precision 0.1cm^{-1} and number of scans was four (4). The spectra were recorded over the wavenumber range of 400-4000 cm^{-1}. The analysis was conducted to identify the characteristic functional groups of lignin and its derivatives and to assess changes across different temperature gradients.

3.2. XRD

The crystal structure of the MCC was investigated using an X-ray diffractometer (SmartLab, Rigaku, Japan) equipped with Cu Kα radiation at a wavelength (λ) of 1.54060 Å. The instrument was operated at 40 kV and 40 mA. Diffraction patterns were recorded over a 2θ range of 10 - 80° using a step size of 0.02°.

The interlayer spacing (d) was calculated by Bragg's law [13]:

$$n\lambda = 2d\sin\theta \tag{i}$$

Where, order of diffraction n (n = 1), X-ray wavelength λ, and Bragg angle θ.

The crystallite size (D) was estimated from the principal diffraction peaks using the Scherrer equation [14]:

$$D = \frac{K\lambda}{\beta\cos\theta} \tag{ii}$$

Where, λ is wavelength of X-ray radiation (λ=1.5406 Å for Cu Kα), K is the shape factor (K=0.9), θ is the Bragg angle, and β is the full width at half maximum intensity of the peak.

The number of stacked graphene layers (N) was calculated as [15, 16]:

$$N = {Lc}/{d_{002}} + 1 \tag{iv}$$

The lattice parameters of the hexagonal cell were determined as [17]:

$$c = 2d_{002} \tag{v}$$

$$a = 2d_{100}\frac{2d_{100}}{\sqrt{3}} \tag{vi}$$

The degree of graphitization (g) was calculated using the Franklin equation [18, 19]:

$$g = {(0.344 - d_{002})}/{(0.344 - 0.3354)} \tag{vii}$$

where 0.344 nm is the interlayer spacing of fully turbostratic carbon and 0.3354 nm is that of ideal graphite [20].

4. Results and Discussion

4.1. FTIR

Figure 1 shows the FTIR peaks of lignin and the heat treatment of lignin in the 100 to 600ºC temperature range. The range of 2800-3000cm^{-1} represents the aliphatic (C-H) group. The peak at 2982cm^{-1} aliphatic groups is present in lignin and other heat-treated lignin. The strong peak range of 1680-1710 cm^{-1} has represented carbonyl groups. In the strong peak 1710cm^{-1} has shown C=O stretching bands from carbonyl

groups (ketones, aldehydes, carboxylic acids) anchored to ester and carboxyl functional groups in lignin, which decrease with rising temperature as oxygenated functionalities are released during pyrolysis. The FTIR peak range 1566-1650cm^{-1} has demonstrated C=C. The 1608cm^{-1} C=C aromatic ring stretching (characteristic of the guaiacyl/syringyl aromatic skeleton), persists to ~400-500°C indicating relative stability of the aromatic core over this range. Strong brand peak 1085-1150cm^{-1} demonstrated an aliphatic ether group. The strong peak at 1127 cm^{-1} C-O-C stretching of ether linkages (particularly β-O-4 aryl ethers), and the dominant inter-unit bonds in native and technical lignin show diminishing intensities with increasing temperature since ether bonds are broken up as part of the coal pyrolysis stage. The strong 624cm^{-1} plane aromatic C-H bending, is lost at high temperature, consistent with condensation followed by graphitization of aromatic structures [21, 22].

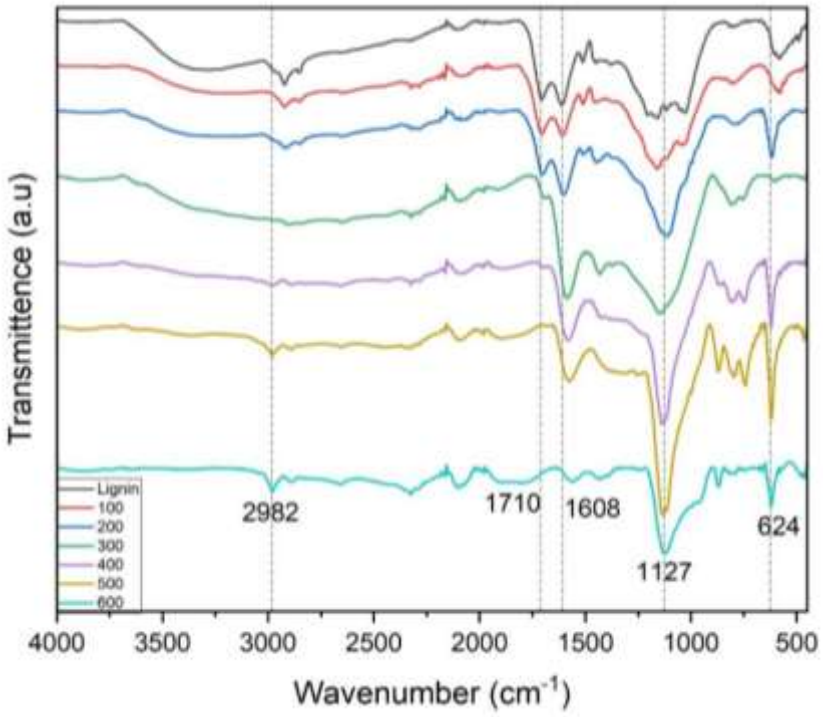

Figure 1. FTIR peak of 0 to 600°C temperature gradient of lignin

The spectra of raw lignin exhibit the most pronounced features, as expected due to the extensive phenylpropanoid network with aliphatic side chains, methoxy, carbonyls and multiple ether linkages. There is a devastating loss of most functional-group bands between about 300-500°C, this range coincides with the first pyrolysis zone, during which β-O-4 and other ether linkages cleave, and side chains are lost. At 600°C FTIR spectra usually reveal heavily attenuated organic functional bands and enrichment in aromatic carbon, signaling the extent of carbonization [21-23].

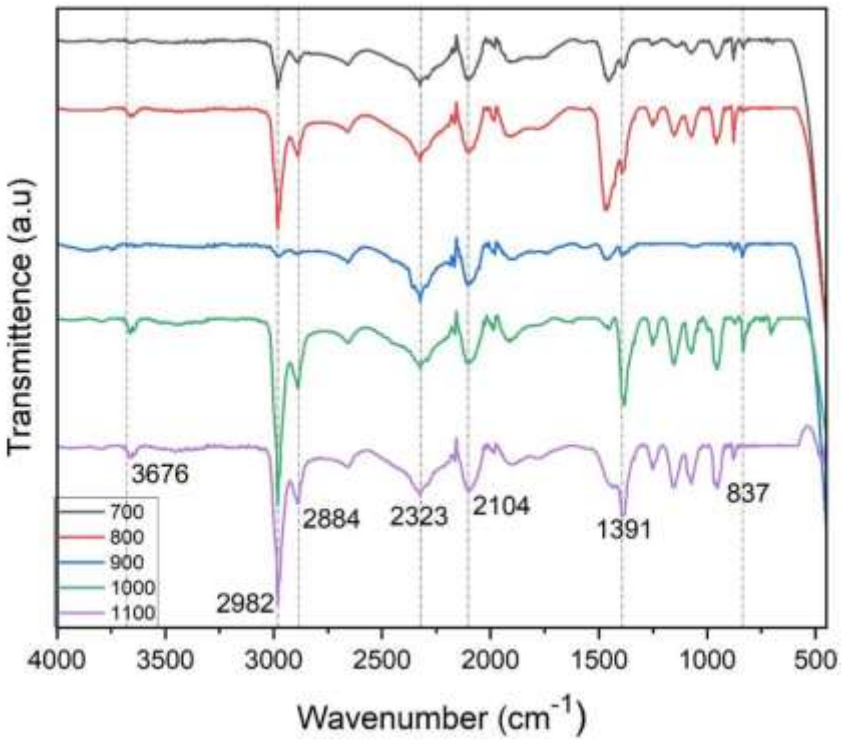

Figure 2. FTIR peak of 700 to 1100°C temperature gradient of lignin

Figure 2 shows the FTIR peaks of lignin and heat treatment of lignin in the 700 to 1100°C temperature range. The range of 2800-3000cm^{-1} represents the aliphatic (C-H) group. The peak at 3676cm^{-1} is the O-H stretch of isolated or free hydroxyl groups, which is rationalized as surface hydroxyls or adsorbed water (moisture) with bands often becoming diminished or disappearing entirely in the ~700-800°C range due to dehydration and structural consolidation. The broad peaks at 2982 and 2884cm^{-1} are residual aliphatic C-H stretching bands that can still be weakly observed in the FTIR spectra at temperatures as high as 700-800°C but have virtually disappeared by 1000-1100°C, consistent with eventual removal of aliphatic groups during heightened carbonization. The peak 2323cm^{-1} typically attributed to CO_2 gas-phase abs. in in-situ/high-temp FTIR or cumulative double-bonded species (C=C=O) evolved during devolatilization. This wavenumber region is generally associated with the evolution of CO_2 during FTIR investigations of biomass and lignin pyrolysis [14, 23-25]. The peak 2104cm^{-1} band in the 2000-2200cm^{-1} region that may indicate C≡C (alkyne) or cumulene-type structures, or in some nitrogen-containing systems C≡N groups, its appearance at elevated temperatures has been associated with creation of sp-hybridized carbon species in lignin-derived carbons 1391cm^{-1} C-H bending of remaining methyls or disorder mode of aromatic/sp^2 carbon precursors, often considered to be linked with defect-rich carbon structures that lay the basis for fully graphitic ordering. In the peak 837cm^{-1} out-of-plane C-H deformation of aromatic rings (probably para-substituted), the durable presence of which implies that condensed aromatic domains remain in effect at 700-1100°C [23, 24, 26].

The temperature range of 700-1100°C represents advanced carbonization during which most aliphatic and oxygen-containing functional groups are removed, and the structure is enriched in aromatic and carbonaceous

structures. We particularly highlight new bands or shoulders between 2100 and 2300cm^{-1} that have been attributed to sp-bonded carbon and other non-graphitic bonding environments intermediate to high-temperature lignin-derived carbons. FTIR spectra of lignin-based carbons become more featureless in classical organic regions above ~1000-1100°C which is consistent with having a predominantly turbostratic carbon structure. Representative original papers on high-temperature lignin-derived carbons and graphitization: hierarchical graphene-like carbons derived from lignin through direct pyrolysis at temperatures up to 1700°C, which report FTIR data and structural transformation evolution, and graphitized biocarbons from lignin formed in solar-driven or catalyst-assisted processes[23, 24].

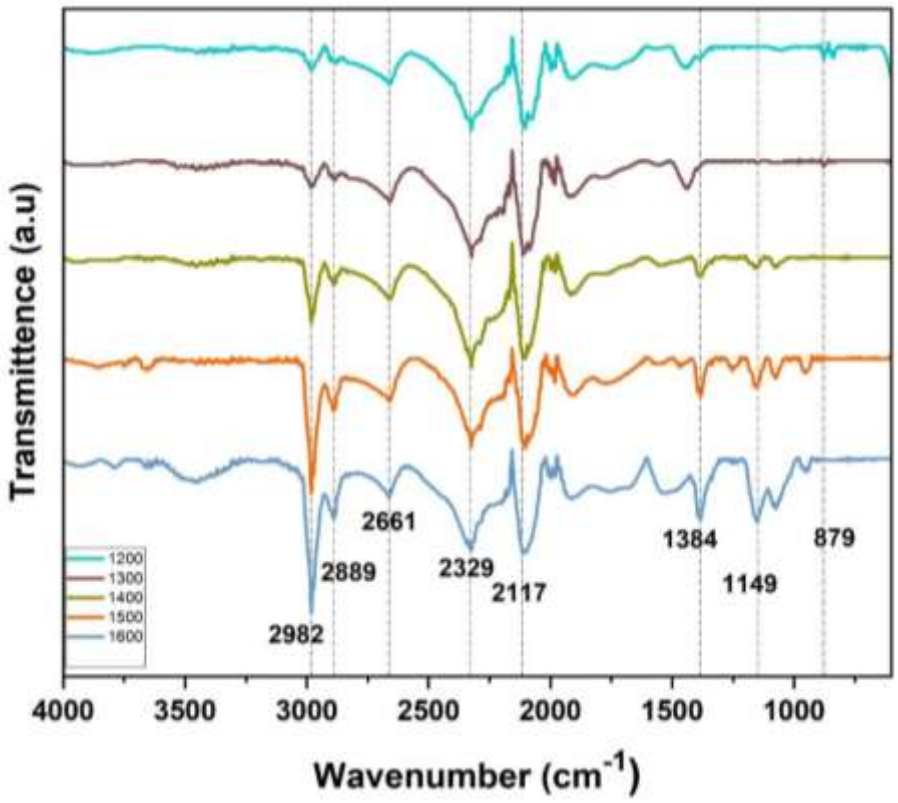

Figure 3. FTIR peak of 1200 to 1600°C temperature gradient of lignin

The strong peaks at 2982 and 2889cm^{-1} traces aliphatic C-H stretching perhaps still visible at 1200-1300°C but vanishing at ≥1400°C, corroborating a virtually total loss of aliphatic carbon in this regime. In the peak of 2661cm^{-1} a somewhat weak feature that can be interpreted as an overtone/combination band, or defect-related sp² features, defect-related overtones in this region have been described for disordered graphitic materials. C=C=O containing species do not contribute to the set values, which are often ascribed to atmospheric or gas-phase CO_2 absorption in high-temperature FTIR. However, on the basis of lignocellulosic pyrolysis, it is expected that CO_2 evolution will continue into high temperatures and arise within this region. The peak 2110cm^{-1} a band characteristic of sp-bonded carbon environments (C≡C) or additional disordered carbon bonding, with its intensity reaching a maximum 1200-1400°C and decreasing once again at

1500-1600°C is in agreement with conversion from polycyclic high sp-content precursors into more structured, ordered graphitic sp^2 domains. The broad band 1384cm^{-1} disordered graphitic carbon, usually observed in FTIR of defect-rich carbons. 1149cm^{-1} weak residual C-O stretching or in-plane C-H bending in condensed aromatic frameworks such low-intensity, minor features can remain in partially graphitized carbons with oxygen-functional surfaces. The peak 879cm^{-1} out-of-plane aromatic C-H or breathing modes of polycyclic aromatic hydrocarbons (PAHs). Stack formation through the growth of larger fused aromatic domains approaches that of graphite/graphene sheets [22, 23, 26].

The FTIR spectra of lignin-derived carbons obtained in the temperature range of 1200-1600°C exhibit only a few weak organic bands, indicating that almost total graphitization has been achieved at these temperatures. The gradual attenuation of the 2110cm^{-1} band past ~1400°C is consistent with sp-hybridized units transitioning into more ordered sp^2 graphitic lattices. At ~ 1600°C the mid-IR region spectra of lignin-derived carbons can be near featureless, a signature of highly graphitic or turbostratic carbon structures. Substantial high-temperature studies: Wang et al. (alkali lignin liquefied at 1700°C, structure featured in a hierarchical graphene-like carbon), solar-driven and catalyst-assisted graphitization of lignin displaying initial acceleration of graphene layer ordering around 1000°C and higher structural order even at ~2000°C, and all other related works on conversion of lignin into graphitic carbon [23, 26].

4.2. XRD

The X-ray diffraction (XRD) pattern of the carbon obtained by pyrolyzing the lignin at 1600°C (Fig. 4) indicates three broad diffraction peaks at 2θ = 25.24°, 43.62° and 78.87° corresponding to the (002), (100)/(101) and (110) planes of hexagonal turbostratic carbon [15, 18, 27, 28]. The absence of a sharp (004) reflection and the absence of clear (101)/(102)/(103) reflections suggest that the graphene-like layers are stacked with random rotational/translational disorder and that it is not graphitic [15, 28-30]. The interlayer spacing (d_{002}) is 0.353 nm, larger than the ideal graphite spacing (0.3354 nm), and the in-plane spacing (d_{100}) is 0.207 nm [18, 27, 29]. The lattice parameters c and a were 0.706 nm and 0.239 nm, respectively. The crystallite stacking height (Lc) and lateral size (La) were ~0.9 nm and ~5 nm, respectively, which corresponds to ~3 stacked layers of graphene [28, 29, 31]. The degree of graphitization (g) was very close to zero, which indicates the non-graphitic, hard-carbon nature of the lignin-derived carbon [18, 29, 32].

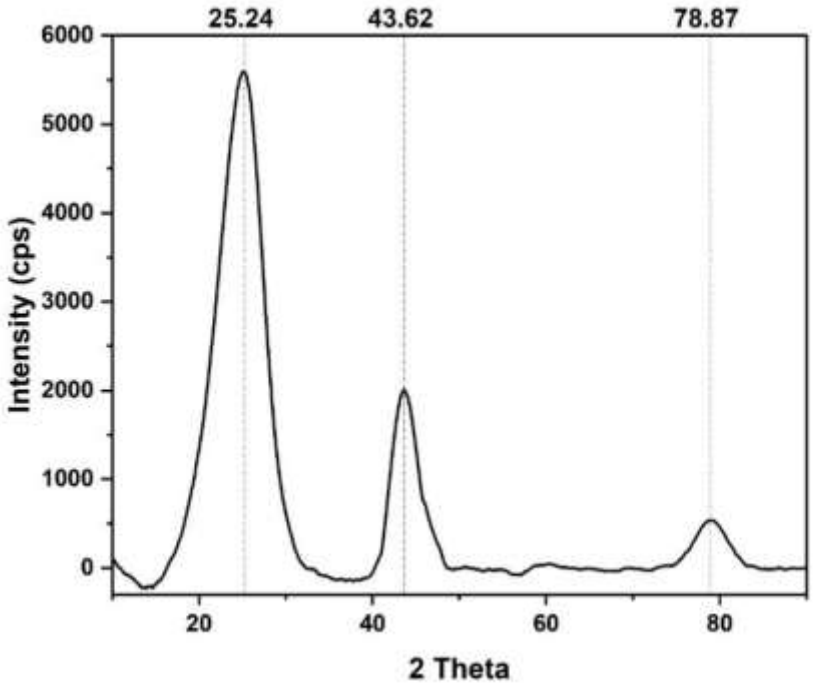

Figure 4. XRD of turbostratic Carbon

5. Yield Amount

The bar chart indicates that the proportion of lignin decreases monotonically over temperatures ranging from 87% at 100ºC to 22% at the maximum temperature, around 1600°C, corroborating the different thermal regimes previously reported elsewhere which targeted lignin pyrolysis and carbonization properties. In the high-yield zone (100-200°C), the mass loss is caused mainly by evaporation of moisture and volatile compounds, producing a sharp drop from 87 to 74% on account of removing weakly bound water and lighter volatiles. The yield decreases sharply from roughly 74 % to 41% as one passes through a fast decomposition region (200-600°C), which correlates with the major pyrolysis stage in which β-O-4 and lignin's central ether linkages are broken, respectively producing largely phenolic vapors along with CO_2, CO, CH_4 and other light gases described in recent mechanistic reviews on lignin pyrolysis. Within the 600-1000°C stabilization region, yield drops more gradually from ~41% to 35%, suggestive of prolonged mass loss as the residual carbon matrix undergoes structural rearrangement and progressive ordering towards a condensed turbostratic carbon scaffold. Already within the 1000-1600°C graphitization window, as heating progresses, yield decreases from ~35% to 22%, a zone where heteroatoms (O, H, N, S) are removed. The carbon framework collapses from disordered aromatic rings towards turbostratic or partially graphitized carbon consistent with reported findings of high-temperature treatment of biomass and lignin-derived hard carbons.

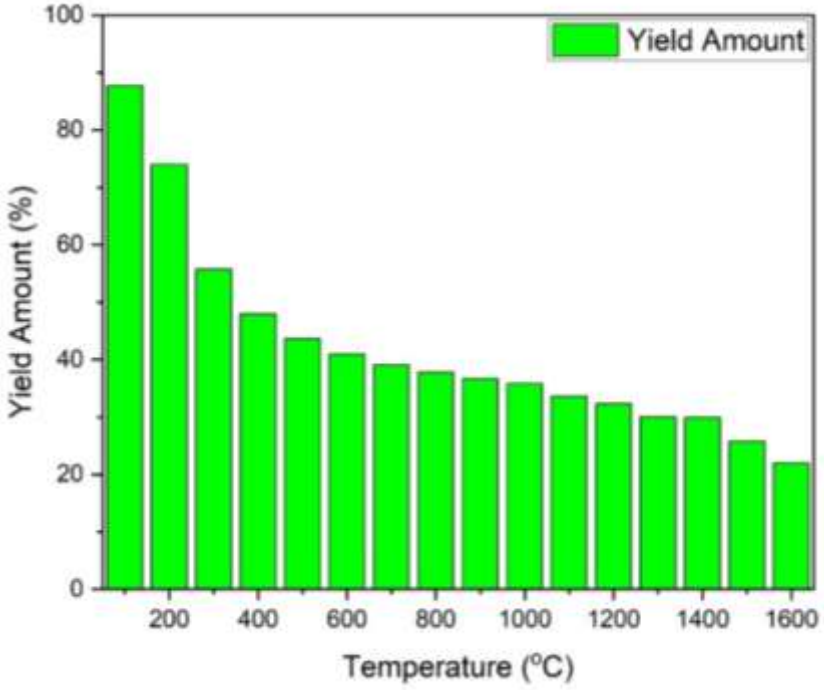

Figure 5. Yield amount of 0 to 1600°C temperature gradient of lignin

In sum, a progressive mass loss pattern between 100 and 1600°C (Figure 4**),** whereas intermediate temperatures exhibited the least pronounced decomposition (from ~200 to 500-600°C), with overall carbon yield seeming to plateau at around 22%, which is competitive over reported yields for char or hard carbon resulting from lignin pyrolysis, and hence is of direct relevance for process parameters that may involve biochar generation, production of precursors for the manufacture of carbon fibre and/or high-temperature treatment of lignin derived carbons for uses in electrochemical energy storage applications [22, 33, 34].

6. Comparation with other Study

Table 1. Comparation with this study and other study

Comparison	Functional Group	Crystal Structure	Yield Amount
Zhang et al. [35] Kraft lignin; 500–1000ºC, Ar	C=O (1705 cm^{-1}), aliphatic C-O (1079, 1030 cm^{-1}), -OH and -CH bands decreased significantly in the range of 200-500ºC; a faint aromatic C=C band (1595 cm^{-1}) was still present at 700-800ºC; and a new band developed around 1458 cm^{-1} at 900-1000ºC.	No (002) peak at 500-600ºC; broad (002) and (10) peaks at 23º and 42º above 700ºC; d_{002} = 0.356 → 0.349 nm; Lc ≈ 0.85 nm; La = 0.7 → 1.4 nm; turbostratic.	91.1% (200ºC) → 44.9% (400ºC); 41% at 500-1000ºC.
Lou et al. [25] Alkali lignin (wheat straw); 1700ºC, N_2	Most of the infrared absorption bands of the original material (-OH ~3530, C-H 2941, aromatic 1600-1400, C-O 1121 and 840 cm^{-1}) were gone from the carbon produced by heating it to 1700ºC.	Sharp (002) peak at 2θ = 26.5º, d_{002} = 0.335 nm; (101-103) planes at d = 0.208-0.217 nm; graphene-like domains with ID/IG = 1.16 (Na/K-catalysed).	30.9% at 1700ºC.
Rigollet et al. [24] Kraft Lignin is pre-carbonized at 800ºC, and then is heated to 1000-2000ºC (with either conventional heating or solar heating)	Not reported (structure assessed by XRD, Raman and HRTEM).	Conventional, 1800ºC: (002) at 24.7º, d_{002} = 0.360 nm, Lc approx. 1.2 nm, La approx. 3.8 nm (turbostratic). Solar, 2000ºC: graphite phase d_{002} = 0.3386 nm (approx. 110 layers), and turbostratic phase d_{002} = 0.3593 nm.	Not reported.
Zhang et al. [36] Enzymatic hydrolysis lignin from corn cobs; stabilized at 200-360ºC, then hot pressed and carbonized at 1000ºC under an argon atmosphere.	At 200°C stabilization, the number of -OH groups reached its peak. After 200°C stabilization, the number of -OH groups decreased. As the stabilization temperature increased, the amount of C-O content decreased, while the amount of C-C content increased (β-O-4 cleavage and cross linking; FTIR/XPS).	The peak position of 2θ = 25.26° (d_{002} = 0.3525 nm, HRTEM ~ 0.345 nm) was obtained for the optimally prepared sample as compared with 2θ = 23.55º for the control.	Stabilization yield 96.1% (200ºC) → 77.5% (320ºC) → 66.1% (360ºC).
This Study	FTIR: 1710 cm^{-1} (C=O), 1608 cm^{-1} (aromatic C=C) and 1127 cm^{-1} (C-O-C) was weakened as the temperature increased; the carbonyl was not present in the sample heated to 600ºC; the aliphatic C-H bands (2982, 2884 cm^{-1}) were almost completely removed when the sample was heated to 1000-1100ºC; the sp-carbon band (2104-2110 cm^{-1}) reached its peak value between 1200-1400ºC, and then decreased in intensity; the spectrum of the sample heated to 1600ºC had very little detail.	At 1600ºC: broad peaks at 2θ = 25.24º, 43.62º, 78.87º [(002), (100)/(101), (110)]; d_{002} = 0.353 nm; Lc ≈ 0.9 nm; La ≈ 5 nm; ~3 layers; g ≈ 0 (turbostratic, non-graphitic).	87% (100ºC) → 74% (200ºC) → 41% (600ºC) → 35% (1000ºC) → 22% (1600ºC).

7. Conclusion

Lignin is collected from lignocellulosic materials using different synthesis methods. Worldwide, an abandoned amount of cotton production for textile product manufacturing is where cotton stalk is mainly used for burning. In this research lignin was extracted from cotton stalk to make valuable products and transform it into derivatives. Lignin FTIR showed a complex phenylpropanoid network, indicating that pure lignin was extracted from the cotton stalk. In this temperature range , the major functional groups of lignin were eliminated at 600°C where the carbonyl group was absent and carbonization aromatic groups formed. In continuity, from 700 to 1100°C aromatic and carbonaceous structures were enriched. At 1200-1600°C major functional groups were formed, and at 1600°C which is like as graphene functional groups and graphite-like statistical functional group phenomena. In this highest temperature region turbostratic carbon forms, which is not fully graphite due to the presence of organic functional groups in this temperature region. In the XRD analysis at 1600ºC represent, the crystal plane and 0.353 nm interlayer spacing (d_{002}) The crystallite stacking height (Lc), lateral size (La), degree of graphitization (g) value close to zero were conformed to the hexagonal turbostratic carbon.

Limitations and future work

In this study, FTIR spectroscopy, XRD and gravimetric yield are used. The spectra were not normalized and no replicates are reported, hence the intensities of the bands are only qualitative and confirmation of bands in the C-H region and between 2000 and 2400 cm-1 are required. There is no Raman data, BET data, SEM data, TGA or NMR data and only a single NaOH concentration (2%) was used, so no effects on the final carbon structure were investigated. Future work will include (i) recording Raman spectra to determine the degree of graphitic order, (ii) measuring of specific surface area and pore structure by N_2 adsorption (BET), (iii) normalizing of FTIR spectra to quantify the relative abundance of the functional groups, (iv) studying the effect of alkali concentration, (v) characterizing the extracted lignin by 2D HSQC NMR and the carbonized samples by solid-state NMR, and (vi) studying the possibility of using catalysts or higher temperatures to increase the degree of graphitic order.

Acknowledgments

The corresponding author would like to thank the Echotex Limited for financial support in performing the research. Finally, expressed gratitude to all co-workers of the project for their kind cooperation during research work.

Funding statement

This research received funding from the “Echotex Limited”, by the corresponding author Dr. Mubarak Ahmad Khan who provided invaluable guidance throughout the entire process, from the research work to the writing of the manuscript.

Author contributions

In this manuscript conceptualization by Dr. Mubarak Ahmad Khan and research work was done Md. Sarwar Jahan. Materials data collection, and analysis by Md. Sarwar Jahan, Md. Latifur Rahman, Faisal S. Rahaman, Samsur Rahaman. The first draft of the manuscript was written by Md. Sarwar Jahan and all authors commented on previous versions of the manuscript. All the authors have read and approved the final manuscript. Dr. Mubarak Ahamd Khan was the corresponding author to do the research work.

Reference

1. Boerjan, W., J. Ralph, and M. Baucher, *Lignin biosynthesis.* Annual review of plant biology, 2003. **54**(1): p. 519-546.
2. Ralph, J., et al., *Lignins: natural polymers from oxidative coupling of 4-hydroxyphenyl-propanoids.* Phytochemistry reviews, 2004. **3**(1): p. 29-60.
3. Silverstein, R.A., et al., *A comparison of chemical pretreatment methods for improving saccharification of cotton stalks.* Bioresource technology, 2007. **98**(16): p. 3000-3011.
4. Calvo-Flores, F.G., et al., *Lignin and lignans as renewable raw materials: chemistry, technology and applications*. 2015: John Wiley & Sons.
5. Feng, P.X., et al., *Bimetallic NiCo Loaded on the Nitrogen-Rich Modified Lignin-Derived Carbon Coordination Network for Accelerated Oxygen Reduction Kinetics.* Rare Metals, 2026. **45**(4): p. e70278.
6. Yang, L., et al., *Effects of sodium carbonate pretreatment on the chemical compositions and enzymatic saccharification of rice straw.* Bioresource technology, 2012. **124**: p. 283-291.
7. Alvarez-Vasco, C., et al., *Unique low-molecular-weight lignin with high purity extracted from wood by deep eutectic solvents (DES): a source of lignin for valorization.* Green chemistry, 2016. **18**(19): p. 5133-5141.
8. Lee, R.A., et al., *Lignin extraction–reassessment of the severity factor with respect to hydroxide concentration.* Bioresource technology, 2014. **169**: p. 707-712.
9. Lengowski, E.C., et al., *Wood Vinegar from Lignocellulosic Biomass in the Context of Forest Biorefineries: Opportunities, Challenges, and Pathways Toward Standardization.* Resources, 2026. **15**(8): p. 110.
10. Feng, P.-X., et al., *Nitrogen-doped lignin mesoporous carbon/nickel/oxide nanocomposites with excellent lithium storage properties: P.-X. Feng et al.* Rare Metals, 2025. **44**(2): p. 889-900.
11. Li, C., et al., *Lignin-stabilized reduced graphene oxide carbon aerogels with tunable dielectric properties for broadband electromagnetic wave absorption, thermal insulation, and infrared stealth.* Journal of Materials Chemistry C, 2026.
12. Liu, Y., et al., *Green electromagnetic shielding materials from biomass: mechanisms, design strategies, and future perspectives.* Advanced Engineering Materials, 2026. **28**(3): p. e202502678.
13. Bragg, W.H. and W.L. Bragg, *X-rays and Crystal Structure*. Vol. 215. 1915: G. Bell and sons, Limited.
14. Jahan, M.S., et al., *Extraction and characterization of cellulose nanocrystals (CNCs) from jute fibers and other by-products towards a circular economy approach.* Materials Circular Economy, 2024. **6**(1): p. 57.
15. Biscoe, J. and B. Warren, *An X-ray study of carbon black.* Journal of Applied Physics, 1942. **13**(6): p. 364-371.
16. Scherrer, P., *Bestimmung der Grösse und der inneren von Kolloidteilchen mittels Röntgenstrahlen Struktur Nachr.* Ges Wiss Göttingen, 1918. **26**: p. 98-100.
17. Bernal, J.D., *The structure of graphite.* Proceedings of the Royal Society of London. Series A, Containing Papers of a Mathematical and Physical Character, 1924. **106**(740): p. 749-773.
18. Franklin, R.E., *Crystallite growth in graphitizing and non-graphitizing carbons.* Proceedings of the Royal Society of London. Series A. Mathematical and Physical Sciences, 1951. **209**(1097): p. 196-218.
19. Franklin, R.E., *The structure of graphitic carbons.* Acta crystallographica, 1951. **4**(3): p. 253-261.
20. Nelson, J. and D. Riley, *The thermal expansion of graphite from 15 c. to 800 c.: part I. Experimental.* Proceedings of the Physical Society, 1945. **57**(6): p. 477-486.
21. Wądrzyk, M., et al., *On mechanism of lignin decomposition–investigation using microscale techniques: Py-GC-MS, Py-FT-IR and TGA.* Renewable Energy, 2021. **177**: p. 942-952.
22. Lu, X. and X. Gu, *A review on lignin pyrolysis: pyrolytic behavior, mechanism, and relevant upgrading for improving process efficiency.* Biotechnology for Biofuels and Bioproducts, 2022. **15**(1): p. 106.
23. De Seram, H., *From lignin to graphitized biocarbon: A sustainable approach for novel materials.* 2023.
24. Rigollet, S., et al., *Synthesis of graphitic biocarbons from lignin fostered by concentrated solar energy.* Scientific Reports, 2025. **15**(1): p. 6418.

25. Lou, R., et al., *Fabrication of hierarchical lignin-based carbon through direct high-temperature pyrolysis and its electrochemical application.* ACS omega, 2021. **6**(49): p. 34129.
26. Lou, R., et al., *Fabrication of hierarchical lignin-based carbon through direct high-temperature pyrolysis and its electrochemical application.* ACS omega, 2021. **6**(49): p. 34129-34136.
27. Li, Z., et al., *X-ray diffraction patterns of graphite and turbostratic carbon.* Carbon, 2007. **45**(8): p. 1686-1695.
28. Warren, B., *X-ray diffraction in random layer lattices.* Physical Review, 1941. **59**(9): p. 693.
29. Puri, B. and P. Walker, *Chemistry and physics of carbon.* Chemistry and Physics of Carbon. Marcel Dekker, New York, 1970: p. 191-282.
30. Goudarzi, A., L.-T. Lin, and F.K. Ko, *X-ray diffraction analysis of kraft lignins and lignin-derived carbon nanofibers.* Journal of Nanotechnology in Engineering and Medicine, 2014. **5**(2): p. 021006.
31. Scherrer, P., *Bestimmung der inneren Struktur und der Größe von Kolloidteilchen mittels Röntgenstrahlen*, in *Kolloidchemie ein lehrbuch*. 1912, Springer. p. 387-409.
32. Glatthaar, C., et al., *Lignin-derived mesoporous carbon for sodium-ion batteries: Block copolymer soft templating and carbon microstructure analysis.* Chemistry of Materials, 2023. **35**(24): p. 10416.
33. Gomez-Martin, A., Z. Schnepp, and J. Ramirez-Rico, *Structural evolution in iron-catalyzed graphitization of hard carbons.* Chemistry of Materials, 2021. **33**(9): p. 3087-3097.
34. Li, W. and J. Shi, *Lignin-derived carbon material for electrochemical energy storage applications: Insight into the process-structure-properties-performance correlations.* Frontiers in Bioengineering and Biotechnology, 2023. **11**: p. 1121027.
35. Zhang, X., et al., *Carbon nanostructure of kraft lignin thermally treated at 500 to 1000 C.* Materials, 2017. **10**(8): p. 975.
36. Zhang, X., et al., *Enhancing the graphitization ability of corn-cob-derived lignin by coupling stabilization and hot-pressing.* RSC advances, 2025. **15**(59): p. 50898-50909.

Appendix

